Nanoscale Res Lett (2010) 5:96–102
DOI 10.1007/s11671-009-9449-9

NANO EXPRESS

Tunable Visible Emission of Ag-Doped CdZnS Alloy Quantum Dots

Ruchi Sethi · Lokendra Kumar · Prashant K. Sharma · A. C. Pandey

Received: 15 July 2009 / Accepted: 24 September 2009 / Published online: 13 October 2009

Abstract Highly luminescent Ag-ion-doped $Cd_{1-x}Zn_xS$ ($0 \leq x \leq 1$) alloy nanocrystals were successfully synthesized by a novel wet chemical precipitation method. Influence of dopant concentration and the Zn/Cd stoichiometric variations in doped alloy nanocrystals have been investigated. The samples were characterized by X-ray diffraction (XRD) and high resolution transmission electron microscope (HRTEM) to investigate the size and structure of the as prepared nanocrystals. A shift in LO phonon modes from micro-Raman investigations and the elemental analysis from the energy dispersive X-ray analysis (EDAX) confirms the stoichiometry of the final product. The average crystallite size was found increasing from 1.0 to 1.4 nm with gradual increase in Ag doping. It was observed that photoluminescence (PL) intensity corresponding to Ag impurity (570 nm), relative to the other two bands 480 and 520 nm that originates due to native defects, enhanced and showed slight red shift with increasing silver doping. In addition, decrease in the band gap energy of the doped nanocrystals indicates that the introduction of dopant ion in the host material influence the particle size of the nanocrystals. The composition dependent bandgap engineering in CdZnS:Ag was achieved to attain the deliberate color tunability and demonstrated successfully, which are potentially important for white light generation.

Keywords Alloy · Nanocrystals · Photoluminescence · Raman spectroscopy

R. Sethi · L. Kumar (✉) · P. K. Sharma · A. C. Pandey
Nanophosphor Application Centre, Physics Department, University of Allahabad, Allahabad 211 002, India
e-mail: lkumarau@gmail.com

Introduction

II–VI compound semiconductor nanocrystals have been paid great attention owing to their unique optical properties that can be tuned not only by changing the particle size but also by changing the composition of the alloy [1–3]. Among them, the wide band gap nanocrystalline materials have opened avenue in fundamental studies and tremendous potential applications in diverse areas such as solar cell, photo-catalysis, sensors, photonic and other opto-electronic devices [4–7]. Toward this end, considerable efforts have been devoted on the high temperature synthesis of $Cd_{1-x}Zn_xS$ ($0 \leq x \leq 1$) nanocrystalline thin films by chemical vapor deposition (CVD), molecular beam epitaxy (MBE), metal organic vapor phase epitaxy (MOVPE) and rf-sputtering method [8–10], but very less attention is paid toward the low temperature chemical synthesis of high quality water soluble alloy nanocrystals. Nanocrystals synthesized by chemical route gives the chance to control their size, distribution and the most important is to improve the crystallinity by altering the concentration of the reagents and their mixing rate at different temperature [11]. These small-size nanostructures have a large surface to volume ratio, which plays a dominant role in optical properties of the nanostructures. For the good quality nanomaterials, various kinds of capping agents and inorganic shell are used to passivate the undesired sites, which results in the enhancement of luminescence intensity. Doping different activator ions (acts as a recombination center) in these stabilized nanostructures not only gives the chance to obtain required emission color, but it also reduces the self quenching by intrinsic defects in the nanocrystals [12]. There are numerous reports on the optical properties of various metal and rare earth ions doped ZnS, CdS, ZnSe, and CdSe nanostructures, but

studies on the their doped alloy nanostructures are still very limited [13–16]. ZnS nanocrystals doped with Ag ion has been paid a great devotion by several researches because of its commercial application as a blue emitting phosphor [17]. In best of our knowledge, there is no report except Karar et al. on the optical properties of the Ag ion doped $Cd_{1-x}Zn_xS$ alloy nanocrystals [18].

In our previous report, the structural and photoluminescence properties of chemically synthesized undoped $Cd_{1-x}Zn_xS$ (0, 0.2, 0.4, 0.6, 0.8 and 1.0) alloy nanocrystals were discussed in detail [19]. It was observed from the obtained results that the XRD peaks are shifted toward higher 2θ values, and the excitation and emission spectra are blue shifted with increasing molar concentration of Zn in alloy. In the present study, for the first time, we have successfully synthesized the Ag-ion-doped $Cd_{1-x}Zn_xS$ ($x = 0$, 0.2, 0.4, 0.6, 0.8 and 1.0) alloy nanocrystals by wet chemical precipitation method and systematically studied the PL properties of doped alloy nanocrystals over all the compositions of Zn and Cd constituents. In addition, effect of dopant concentration on the PL intensity of alloy nanocrystals has been also studied and explained. Raman investigation and absorption measurements were also performed to confirm the formation of doped alloy nanocrystals.

Experimental

Zinc acetate ($Zn(CH_3COO)_2{\cdot}2H_2O$), cadmium acetate ($Cd(CH_3COO)_2{\cdot}2H_2O$), urea ($NH_2CONH_2$), silver nitrate ($AgNO_3$), triethylamine ($N(CH_2CH_3)_3$) were purchased from Merck India Limited and thiourea (NH_2CSNH_2) was purchased from RENKEM. All chemicals were of analytical grade and used as received without any further purification. Milli-Q water was used as a solvent for all chemical reactions. Nanocrystals were prepared using a simple chemical co-precipitation method as reported by Chawla et al. with minor modifications in the reaction conditions [20]. The detailed description of the experimental procedure is described as follows: firstly appropriate amount of zinc acetate and cadmium acetate (according to their molar ratio as required for the particular composition) was dissolved in 25 ml of water to make 0.5 M solution named solution A. To make the sulfur solution, 1 M thiourea, 1 M urea and 2 ml triethylamine (TEA) were dissolved in 25 ml water named solution B. Both the solutions were stirred until a colorless transparent solution obtained. TEA was used in the chemical reaction because it makes a complex with Zn and Cd ion and reduces their solubility product difference and urea to control the pH of solution. Doping of Ag ion was achieved by adding the calculated amount of $Ag(NO_3)_2$ (0, 2, 4, 8, 12 and 15 M%) in the initial solution A. Solution B was kept at hot plate magnetic stirrer at 70°C temperature and then solution A was added drop wise in solution B @ 1 ml/min with keeping the stirring on. The color of obtained precipitate changes from white to deep yellow by varying the ratio of Cd and Zn in the starting solution. Finally the precipitate was centrifuged, washed with water and ethanol several times and then dried in vacuum oven at 100°C to obtain the powder nanocrystals for the characterization purpose.

To calculate the particle size and structure of the nanocrystals, X-Ray diffraction was carried out on Rigaku D/max-2200 PC diffractometer operated at 40 kV/20 mA using CuK_α radiation with wavelength of 1.54 Å in the wide angle 2θ range from 10 to 60°. Technai 30 G^2 S-Twin high resolution transmission electron microscope (HRTEM) operated at 300 KV was used to obtain the particle size and electron diffraction image. For TEM, sample was prepared by suspending the $Cd_{0.4}Zn_{0.6}S$:Ag (8 M % of Ag ion) powder in ethanol and depositing a drop of this ethanolic solution onto the carbon coated copper grid and then dried it at room temperature. Photoluminescence (PL) measurement was carried out using Perkin Elmer LS-55 Luminescence spectrophotometer, while Perkin Elmer Lambda-35 was used to measure UV–vis absorption spectra. A Renishaw micro-Raman spectrometer (Model-2000, $\lambda = 514$ nm) integrated with nanonics atomic force microscopy (AFM) is used to investigate the optical phonon modes of the synthesized nanopowder. Raman spectrum is recorded by selecting 20X objective of integrated Lica microscope with the spot size 20 μm.

Results and Discussion

Effect of alloy composition on the XRD spectra is already reported in our previous article [19]. Figure 1 shows the XRD profile of $Cd_{0.4}Zn_{0.6}S$:Ag nanocrystals with different Ag ion concentration (0, 2, 4 and 8 M% of Ag ion). X-ray diffraction pattern of the samples exhibit peaks centered at 27.37, 44.42 and 53.29°, which correspond to cubic structure of the nanocrystals with three most preferred orientations along the (111), (220) and (311) planes. The peaks are well matched with the standard Joint Committee on Powder Diffraction Standard (JCPDS) file. XRD confirms the phase singularity of the synthesized material, i.e. no other peak is observed corresponding to their binary system or the silver impurity, which confirms the formation of alloy nanocrystals rather than their separate nucleation or phase formation. Broad diffraction peaks confirm the nanocrystalline nature of the particles and can be used to calculate the average crystallite size by Debye Sherrer equation [21]

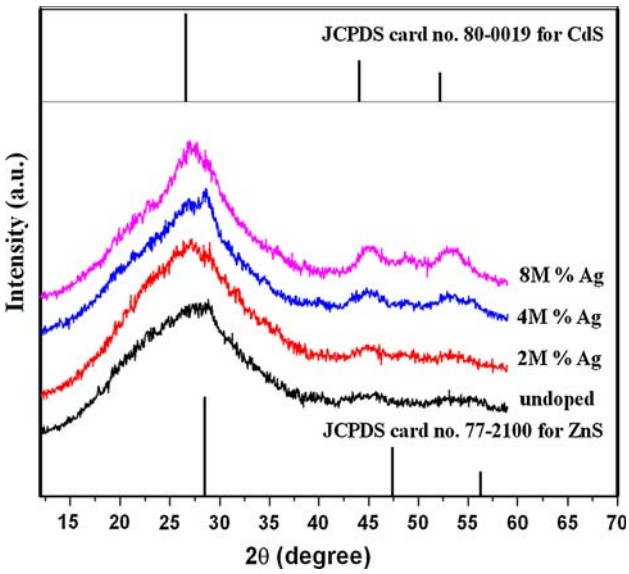

Fig. 1 XRD spectra of $Cd_{0.4}Zn_{0.6}S$:Ag quantum dots for different composition of Ag ion impurity (0, 2, 4 and 8 M %). Standard JCPDS files for cubic CdS and ZnS are shown on the top and bottom of the X-axis, respectively

$$size = \left\{ \frac{0.9 \times \lambda}{FWHM \times \cos(\theta)} \right\} \quad (1)$$

where λ is the wavelength used in XRD, θ is Bragg angle and FWHM is full width of half maxima at 2θ angle. The estimated crystallite size of the nanocrystals using the above equation (1) is found to be increased from 1.0 to 1.4 nm with increasing Ag ion concentration. The increase in particle size is also clear from the decrease in the FWHM of the XRD peaks.

Figure 2 shows the transmission electron micrograph (TEM) and selected area electron diffraction (SAED) pattern of $Cd_{0.4}Zn_{0.6}S$:Ag (8 M % of Ag ion) nanocrystals. TEM image reveals that the particles are spherical in shape having diameter less than 5 nm. Homogeneous distribution of the nanocrystals is also confirmed by HRTEM as shown in Fig. 2b. SAED pattern (inset of Fig. 2a) and well-resolved lattice fringes (interplanar spacing 'd' = 3.1 Å) obtained in HRTEM (inset of Fig. 2b) indicate the formation of the cubic structure and crystalline nature of the particles, respectively. These results are consistent with the results obtained from the XRD spectra. We have also

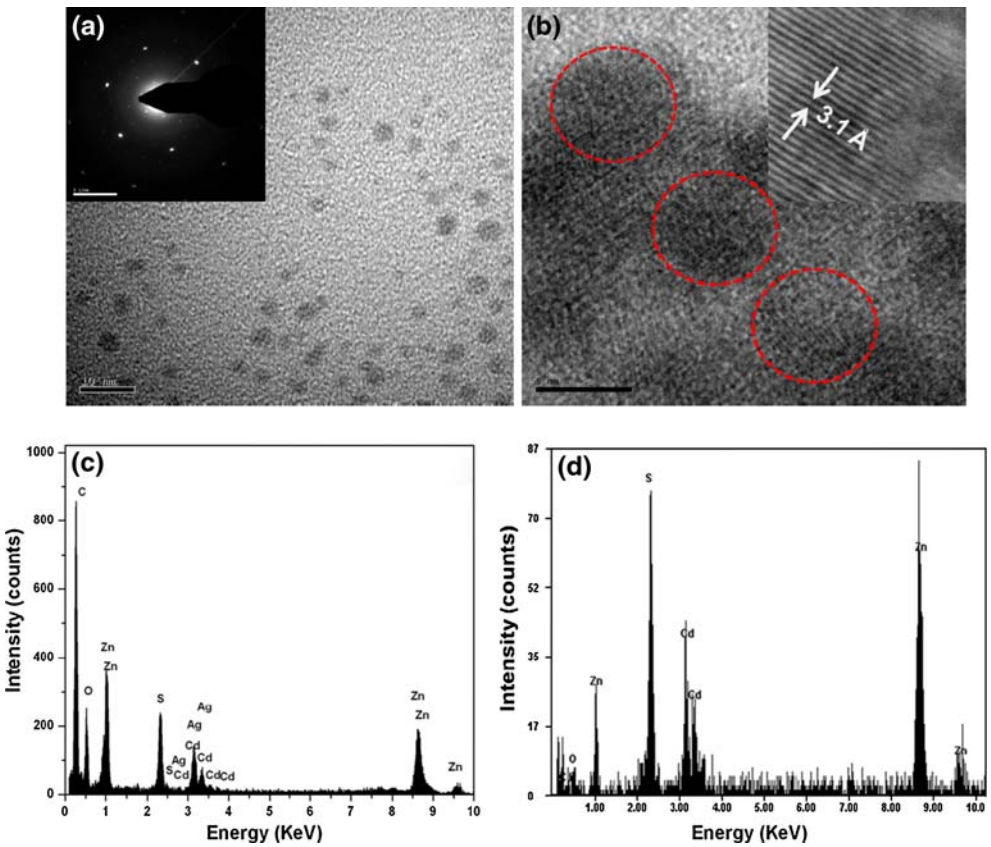

Fig. 2 TEM image of **a** $Cd_{0.4}Zn_{0.6}S$:Ag nanocrystals and **b** corresponding HRTEM image. Inset of **a** and **b** represents their corresponding SAED and interplanar spacing'd'. Representative EDX spectra of doped alloy nanocrystals are shown in **c**, whereas for undoped sample, the EDX is given in **d**

performed the energy dispersive X-ray analysis (EDAX) for undoped and doped (8 M % Ag) $Cd_{0.4}Zn_{0.6}S$ system for the compositional analysis as shown in Fig. 2c, d, respectively. From the EDAX analysis, it is confirmed that stoichiometric of the Zn, Cd and Ag constituent is maintained in the finally prepared nanocrystals. From the EDAX line traces, the presence of Ag ion into the crystal structure of $Cd_{0.4}Zn_{0.6}S$ can also be concluded. The peaks of C and O are from the carbon coated copper grid substrate used for the sample preparation.

Figure 3 shows the micro-Raman spectroscopic graph for the investigation of vibrational properties of $Cd_{0.4}Zn_{0.6}S$:Ag (8 M % of Ag ion) nanopowder. Ar^+ ion laser source with excitation wavelength 514 nm is used to excite the material. Raman spectra of the samples show two broad asymmetric peaks correspond to the scattering from 1LO and 2LO phonon modes [22]. Shift in the peak position and asymmetric broadening toward lower frequency side appears in the nanocrystals compared to their bulk material, which is due to the relaxation of the fundamental selection rule $q \sim 0$ (where q is the scattering vector) and allows the participation of phonon away from the brillouin zone center to contribute in Raman scattering [23, 24]. No peak is observed corresponding to scattering from silver sulfide phase, which confirms the doping of Ag ion in the host nanocrystals. Position of 1LO phonon peak ($\sim$319 cm^{-1}) deduced from Raman spectrum of $Cd_{0.4}Zn_{0.6}S$ is shifted toward higher wave number side in comparison with the 1LO phonon peak position for CdS ($\sim$297 cm^{-1}) [22] nanocrystals, which substantiates the formation of alloy nanocrystals. We have not observed any appreciable shift in Raman spectra of doped sample in comparison with the undoped one.

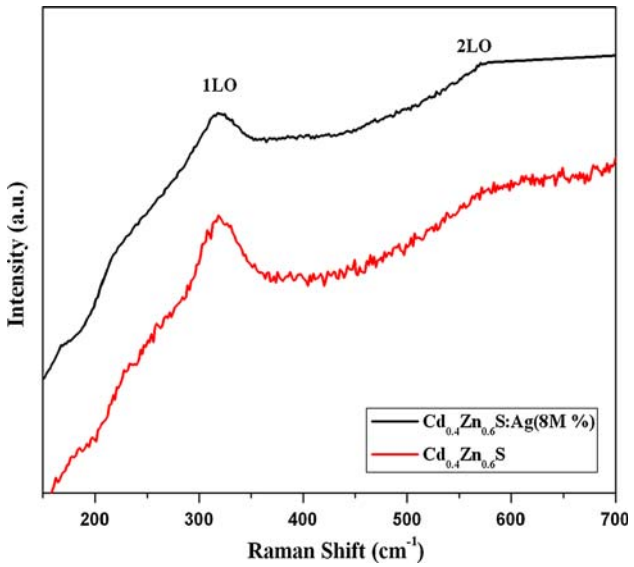

Fig. 3 Raman spectra of the undoped and Ag doped $Cd_{0.4}Zn_{0.6}S$ alloy nanocrystals with excitation wavelength 514 nm

Figure 4 shows the photographs of doped and undoped $Cd_{0.4}Zn_{0.6}S$ nanocrystals under the UV lamp. Figure 4a shows the color of as prepared nanocrystals in the ordinary light, whereas photographs shown in Fig. 4b, c correspond to the bright green and bright orange-red color luminescence from the undoped and Ag-ion-doped samples, respectively, under UV illumination (365 nm). Optical absorption measurement for $Cd_{0.4}Zn_{0.6}S$:Ag (2, 4, 8 M % of Ag ion) nanocrystals are shown in Fig. 5. Absorption peak position at about 368 nm is blue shifted corresponding to their bulk counterparts and reveals the nanocrystalline nature of the particles. A red shift of 10 nm in the absorption band is also found with increasing the content of Ag ion in the alloy nanocrystals [25]. This shift in absorption spectra appears due to the increase in particle size with the substitution of comparatively larger radii Ag ion in the host material. The results obtained from the UV–Vis spectroscopy are consistent with the XRD results. Absorption spectra do not show any additional band and rules out any extra phase formation in the alloy nanocrystals.

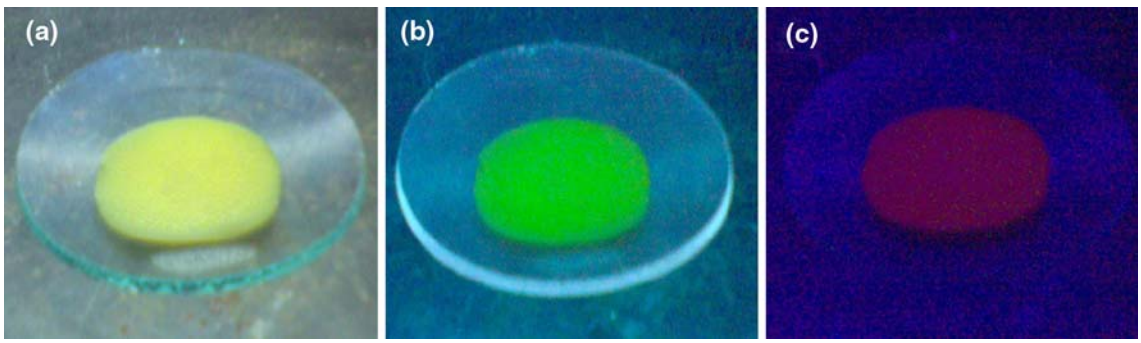

Fig. 4 Photographs of the synthesized material **a** in ordinary lamp **b** green emission from undoped $Cd_{0.4}Zn_{0.6}S$ nanocrystals under UV excitation and **c** orange emission from doped $Cd_{0.4}Zn_{0.6}S$:Ag (8 M %) nanocrystals under UV lamp (excitation wavelength 365 nm)

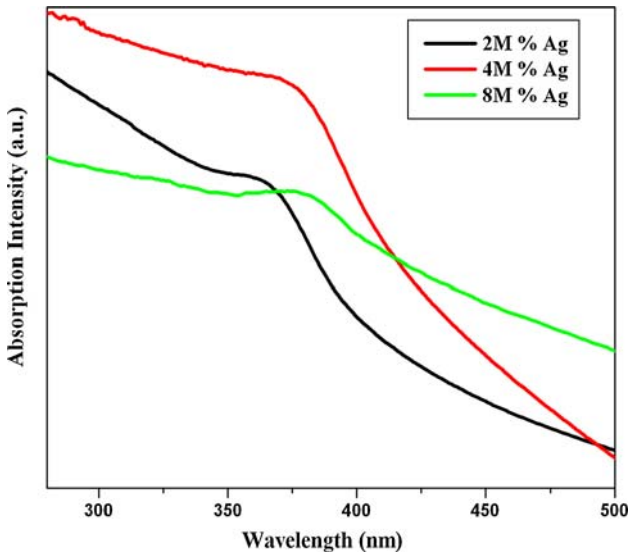

Fig. 5 Optical absorption spectra of silver ion doped $Cd_{0.4}Zn_{0.6}S$ nanocrystals for different doping concentration (2, 4, 8 M%)

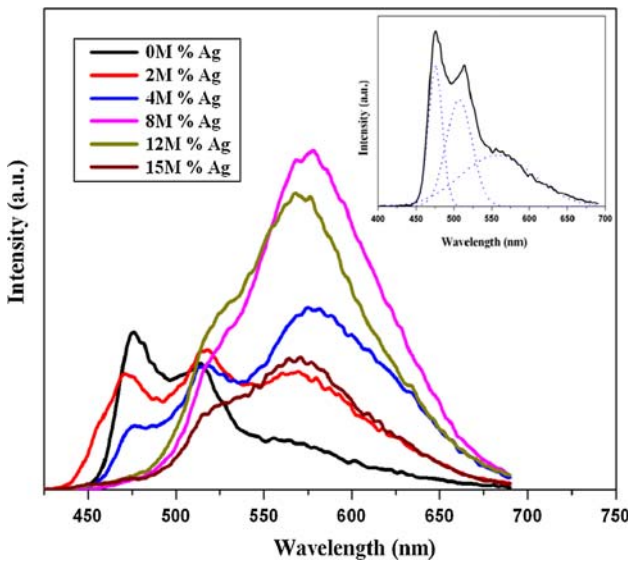

Fig. 6 Room Temperature PL spectra of the $Cd_{0.4}Zn_{0.6}S$:Ag nanocrystals recorded at 350 nm excitation wavelength. Concentration of Ag ion (0, 2, 4, 8, 12, 15 M %) significantly affects the intensity ratio of defect related transition and dopant related transition. Inset shows the Gaussian fitted deconvoluted spectra for undoped nanocrystals

Room temperature PL spectra of $Cd_{0.4}Zn_{0.6}S$ nanocrystals with different Ag ion concentration (0, 2, 4, 8, 12, 15 M % of Ag ion) are shown in Fig. 6. The measurements have been performed at an excitation wavelength of 350 nm. PL spectra for the undoped nanocrystals of $Cd_{0.4}Zn_{0.6}S$ show a broad asymmetric peak, which implies the superposition of multiple emission bands. The spectra are fitted with Gaussian curve fitting, which results in the three emission bands centered at 480, 520 and 558 nm. From the UV–Vis measurement, it is obvious that above transitions do not belong to a band edge emission, since these emission bands are largely red shifted from the absorption edge. These transitions belong to the native defects produced in the nanocrystals due to very small size. Emission peak at 480 nm can be attributed to the transition from the shallow trap level, while peak at 520 nm can be assigned to the radiative transition from the deep trap states due to the sulfur vacancy. This was confirmed by performing the similar experiment for the undoped nanocrystals with the different content of sulfur ions (figure not shown here). The peak intensity corresponding to 480 and 520 nm was found decreasing with increasing amount of sulfur [26]. So it is suggested that the PL peak belongs to the transition from the sulfur vacancies, which reduces with increasing sulfur content in the chemical reaction. PL peak position at 558 nm belongs to the radiative transition from the sulfur vacancy to the interstitial sites created by Zn and Cd ions in the alloy [27]. No additional impurity phase is observed for the undoped sample, confirmed by EDAX measurements. For the silver-ion-doped $Cd_{0.4}Zn_{0.6}S$ nanocrystals, an additional strong emission band emerges at 570 nm that can be ascribed to the recombination of electron trapped near the conduction band and the hole trapped in the level of doped Ag impurity always lie near the valance band. We have also performed the similar experiment for the different concentration of Ag doping (keeping the composition of alloy is fixed i.e. $Cd_{0.4}Zn_{0.6}S$) and studied the influence of dopant concentration on the emission intensity of the nanocrystals. A continuous increase in the emission peak intensity is observed, which is slightly red shifted ($\sim$10 nm) with the increasing concentration of Ag ion upto an optimum concentration (in our case 8 M %). At this concentration, the emission that belongs to the Ag impurity is completely dominated over the defect-related transition. The observed red shift in the emission band with increasing doping concentration can be explained by the increased particle size with doping concentration (confirmed by XRD and UV–Vis characterization). Change in particle size with increase in doping concentration has also been observed by Geng et al. and Ye et al. for the $ZnS:Cu^{2+}$ and ZnO:Ga nanocrystals, respectively [28, 29]. If we further increase the doping concentration above this value, the intensity of the Ag related emission suddenly drops and can be interpreted as the effect of the concentration quenching [30, 31].

To see the effect of stoichiometry variation in the optical property of doped CdZnS alloy nanocrystals, we have synthesized $Cd_{0.0}Zn_{1.0}S$, $Cd_{0.2}Zn_{0.8}S$, $Cd_{0.4}Zn_{0.6}S$, $Cd_{0.6}Zn_{0.4}S$, $Cd_{0.8}Zn_{0.2}S$ and $Cd_{1.0}Zn_{0.0}S$ alloy composition with a fixed concentration of Ag dopant (8 M %). Photoluminescence spectra of $Cd_{1-x}Zn_xS$:Ag alloy

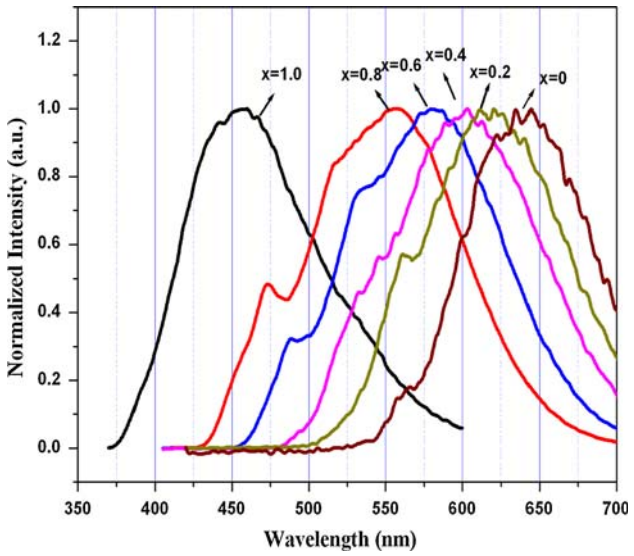

Fig. 7 PL spectra recorded for the Ag ion (8 M %) doped $Cd_{0.0}Zn_{1.0}S$, $Cd_{0.2}Zn_{0.8}S$, $Cd_{0.4}Zn_{0.6}S$, $Cd_{0.6}Zn_{0.4}S$, $Cd_{0.8}Zn_{0.2}S$ and $Cd_{1.0}Zn_{0.0}S$ alloy nanocrystals corresponding to their band edge excitation wavelength

nanocrystals are recorded by photoluminescence spectrophotometer as shown in Fig. 7. A red shift (from blue region to red region) in PL peak position is observed with increasing the Cd content in the Ag-doped CdZnS alloy nanocrystals. We have also performed the PL measurements for the undoped $Cd_{1-x}Zn_xS$ $(0 \leq x \leq 1)$ alloy nanocrystals and observed that the emission peak shift from blue to green region [19]. PL spectra for the undoped nanocrystals arise from the transition of electron trapped in the sulfur vacancy to the valance band, while for doped samples PL spectra can be attributed to the localized energy level introduced by the dopant ion, which acts as an acceptor impurity, and the emission arises from the electron transition from the sulfur vacancy to the Ag dopant impurity level. Increasing stoichiometric ratio of Cd/Zn in the alloy nanocrystals reduces the band gap energy of the ternary system. (according to vegard's empirical quadratic equation $E_{.g.} = 2.42 + 0.9\ x + 0.3\ x^2$) [32]. Any change in the position of donor and acceptor level introduced by the native defects, and impurity ions depends on the composition of the alloy. It is also observed by Gross et al. in 1959 that the energy difference between the various states associated with luminescence process are shown to decrease monotonically as the forbidden band gap is decreased with increasing Cd concentration in bulk CdZnS:Ag crystals [33]. Since the energy level of Ag impurity always lie near the valance band within the band gap, therefore, any change in the valance band position with composition will also shift the position of Ag level in accordance with the Gross et al. and results in the emission tunability in the PL spectra.

Conclusion

Synthesis of high quality luminescent and free standing $Cd_{1-x}Zn_xS$ $(0 \leq x \leq 1)$ nanocrystals doped with Ag ion is first time reported by chemical precipitation method. We have systematically examined the photoluminescence properties for a fixed composition of alloy with varying amount of Ag doping concentration. Doping concentration significantly improved the emission intensity corresponding to the dopant ion up to an optimum concentration. X-ray diffraction and UV–Vis absorption spectra show the increase in particle size with increasing doping concentration. HRTEM image reveals the crystalline nature of the particle having cubic structure with average grain size less than 5 nm. Absorption and Raman investigation confirms the formation of alloy nanocrystals. For the fixed Ag ion doping concentration, the PL spectra of the samples show the emission tunability in full visible range with the change in composition of the alloys and can be used for the white light generation.

Acknowledgments We are grateful to Professor R. N. Bhargava, Nano Crystal Technology, New York (USA) for continuous encouragements and scientific discussions. One of the authors Ruchi Sethi would like to thank, Mr. Ashish K. Keshari Nanophosphor Application Centre, Physics Department, University of Allahabad, India for XRD measurements. Department of Science and Technology, New Delhi, India is thankfully acknowledged for financial support to "Nanophosphor Application Centre" project under 'IRHPA'scheme.

References

1. R.E. Bailey, S. Nie, J. Am. Chem. Soc. **125**, 7100 (2003). doi:10.1021/ja035000o
2. X. Zhong, Y. Feng, W. Knoll, M. Han, J. Am. Chem. Soc. **125**, 13559 (2003). doi:10.1021/ja036683a
3. J. Cizeron, M.P. Pileni, J. Phys. Chem. **99**, 17410 (1995). doi:10.1021/j100048a016
4. J.H. Lee, W.C. Song, J.S. Yi, K.J. Yang, W.D. Han, J. Hwang, Thin Solid Films **431**, 349 (2003). doi:10.1016/S0040-6090(03)00526-1
5. B.J. Wu, H. Cheng, S. Guha, M.A. Haase, J. Depuydt, G. Meishaugen, J. Qui, Appl. Phys. Lett. **63**, 2935 (1993). doi:10.1063/1.110278
6. P.K. Sharma, R.K. Dutta, M. Kumar, P.K. Singh, A.C. Pandey, J. Lumin. **129**, 605 (2009). doi:10.1016/j.jlumin.2009.01.004
7. A.K. Keshari, A.C. Pandey, J. Appl. Phys. **105**, 064315 (2009). doi:10.1063/1.3086617
8. S. Yamaga, A. Yoshikawa, H. Kasai, J. Cryst. Growth **99**, 432 (1990)
9. K. Yamaguchi, S. Sato, Jpn. J. Appl. Phys. **23**, 126 (1984). doi:10.1143/JJAP.23.126
10. T. Karasawa, K. Ahkawa, T. Mitsuyum, J. Appl. Phys. **69**, 3226 (1991). doi:10.1063/1.348541
11. R. Rossetti, R. Hull, J.M. Gibson, L.E. Brus, J. Chem. Phys. **82**, 552 (1985). doi:10.1063/1.448727
12. Q. Xiao, C. Xiao, Appl. Surface Sci. **254**, 6432 (2008). doi:10.1016/j.apsusc.2008.04.002

13. N. Karar, F. Singh, B.R. Mehta, J. Appl. Phys. **95**, 656 (2004). doi:10.1063/1.1633347
14. D. Haranath, N. Bhalla, H. Chandra, Rashmi, M. Kar, R. Kishore, J. Appl. Phys. **96**, 6700 (2004). doi:10.1063/1.1806552
15. D.R. Jung, D. Son, J. Kim, C. Kim, B. Park, Appl. Phys. Lett. **93**, 163118 (2008). doi:10.1063/1.3007980
16. W. Wang, F. Huang, Y. Xia, A. Wang, J. Lumin. **128**, 610 (2008). doi:10.1016/j.jlumin.2007.10.003
17. A. Murugadoss, A. Chattopadhay, Bull. Mater. Sci. **31**, 533 (2008)
18. N. Karar, M. Jayaswal, S.K. Halder, H. Chandra, J. Alloys and Compounds **436**, 61 (2007). doi:10.1016/j.jallcom.2006.07.039
19. R. Sethi, L. Kumar, A.C. Pandey, J. Nanosci. Nanotechnol. **9**, 5329 (2009). doi:10.1166/jnn.2009.1153
20. K. Jayanthi, S. Chawla, H. Chandra, D. Haranath, Cryst. Res. Technol. **42**, 976 (2007). doi:10.1002/crat200710950
21. B.D. Cullity, *Elements of X-Ray diffraction* (Addision-Wesley, Reading, MA, 1978)
22. S. Sahoo, S. Dhara, V. Sivasubramanian, S. Kalavathi, A.K. Arora, J. Raman Spectrosc. **40**, 1050 (2009) doi:10.1002/jrs.2232
23. Y.Y. Luo, G.T. Duan, G.H. Li, Appl. Phys. Lett. **90**, 201911 (2007). doi:10.1063/1.2737398
24. R.R. Prabhu, M.A. Khadar, Bull. Mater. Sci. **31**, 511 (2008)
25. Z. Jindai, N.K. Verma, J. Mater. Sci. **43**, 6539 (2008). doi:10.1007/s10853-008-2818-4
26. K. Manzoor, S.R. Vadera, N. Kumar, T.R.N. Kutty, Mater. Chem. Phys. **82**, 718 (2003). doi:10.1016/S0254-0584(0300366-3)
27. W.Q. Peng, G.W. Cong, S.C. Qu, Z.G. Wang, Opt. Mater. **29**, 313 (2006). doi:10.1016/j.optmat.2005.10.003
28. B. Geng, J. Ma, F. Zhan, Materials Chemistry and Physics **113**, 534 (2009). doi:10.1016/j.matchemphys.2008.08.006
29. Z.Z. Ye, Y.J. Zeng, Y.F. Lu, S.S. Lin, L. Sun, L.P. Zhu, B.H. Zhao, Appl. Phys. Lett. **91**, 112110 (2007). doi:10.1063/1.2784198
30. S. Kar, S. Bisbas, S. Chaudhari, P.M.G. Nambissan, Nanotechnology **18**, 225606 (2007). doi:10.1088/0957-4484/18/22/225606
31. K. Sooklal, B.S. Cullum, S.M. Angel, C.J. Murphy, J. Phys. Chem. **100**, 4551 (1996). doi:10.1021/jp952377
32. V. Akdogan, C. Uzum, O. Dag, N. Coombs, J. Mater. Chem. **16**, 2048 (2006). doi:10.1039/b602584f
33. G.E. Gross, Phys. Rev. **116**, 1478 (1959)